HETE-2 observation of the evidence of a long acting engine in the extremely soft XRF 040916

Makoto Arimoto*, Nobuyuki Kawai*, Motoko Suzuki†, Rie Sato*, Nicolas Vasquez Pazmino*, Takashi Shimokawabe*, Takuto Ishimura*, Yujin E. Nakagawa**, Alexandre Pelangeon‡, Jean-Luc Atteia‡, Kevin Hurley§, Graziella Pizzichini¶ and Donald Q. Lamb‖

*Department of Physics, Tokyo Institute of Technology, 2-12-1 Ookayama, Meguro-ku, Tokyo 152-8551
†JAXA, 2-1-1 Sengen, Tsukuba, Ibaraki, 305-8505
**Department of Physics and Mathematics, Aoyama Gakuin University, 5-10-1 Fuchinobe, Sagamihara, Kanagawa 229-8558
‡LATT, Observatoire Midi-Pyrénées (CNRS-UPS), 14 Avenue E. Belin, 31400 Toulouse, France
§Space Sciences Laboratory, University of California, Berkeley, California, 94720-7450
¶INAF/IASF Bologna, Via Gobetti 101, 40129 Bologna, Italy
‖Deparment of Astronomy and Astrophysics, University of Chicago, 5640 South Ellis Avenue, Chicago, Illinois 60637, USA

Abstract. A long and extremely soft X-ray flash was detected and localized by the instruments aboard the *HETE-2* at 00:03:30 UT on 2004 Sep. 16. This burst consists of two peaks separated by ∼200 s, with durations of about 110 s and 60 s. We have analyzed the energy spectra of the 1st and 2nd peaks observed with the Wide Field X-Ray Monitor (WXM) and the French Gamma Telescope (FREGATE). We discuss the origin of the 2nd peak in terms of flux variabilities and timescales. We find that it is most likely part of the prompt emission, and is explained by the long-acting engine model.

Keywords: gamma-rays: bursts — X-rays: bursts — X-rays: individual (XRF040916)
PACS: 98.70.Qy, 98.70.Rz

INTRODUCTION

Swift has detected early X-ray afterglows with the XRT and bright X-ray flares 100−1000 seconds after the prompt emission for many bursts. They have been explained by the long-acting engine model [1]. In this paper, we report the detection and localization of XRF 040916 by the *HETE-2* satellite and present the results of a detailed temporal and spectral analysis. Since this burst has two peaks within a total time interval of ∼350 s, we discuss the origin of the long timescale [2].

OBSERVATION

XRF 040916 triggered the WXM on 2004 September 16, at 00:03:30 UT. This burst consists of two peaks lasting about 110 s and 60 s separated by a time interval of ∼200 s. This position was reported in the GRB Coordinates Network (GCN) Position Notice [3]. The detection of the optical afterglow was first reported by [4], who found it at

CP1000, *Gamma-Ray Bursts 2007: Proceedings of the Santa Fe Conference*, edited by M. Galassi, D. Palmer, and E. Fenimore

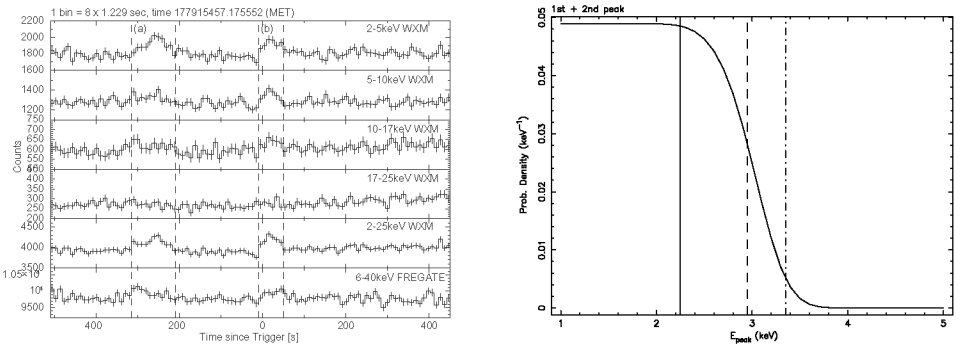

FIGURE 1. (Left): Light curve of XRF 040916. The regions (a) and (b) are the foregrounds of the 1st and 2nd peak respectively. (Right):Posterior probability density distribution for the entire burst of $E^{\rm obs}_{\rm peak}$ using the *constrained* Band function. The vertical solid lines define the 68% probatility interval for $E^{\rm obs}_{\rm peak}$, while the dashed and dotted lines show the 95% and 99.7% probability upper limits on $E^{\rm obs}_{\rm peak}$.

R.A. = $23^{\rm h}00^{\rm m}55^{\rm s}.13$, Dec. = $-5^{\rm d}38'43''.2$ using SuprimeCam on the prime-focus of the Subaru 8.2m telescope. The afterglow was detected in the z', I_c, R_c, V and B-bands in this observation. Despite these observations, no redshift has been determined.

Figure 1 (left) shows the light curve of XRF 040916 in five WXM energy bands (2−5, 5−10, 10−17, 17−25, and 2−25 keV). There are two peaks in the WXM bands and no significant emission above 17 keV.

For spectral analysis, this burst seems to be extremely soft, and if $E^{\rm obs}_{\rm peak}$ is near the low-energy threshold, the spectrum will appear to follow a power-law, even if it is actually a Band function. In such situation, We can constrain $E^{\rm obs}_{\rm peak}$ using a *constrained* Band function [5]. Applying the *constrained* Band function model to this burst, we obtained a constrained $E^{\rm obs}_{\rm peak}$. The result is shown in Figure 1 (right) as the posterior probability density distribution for $E^{\rm obs}_{\rm peak}$. From these distributions, we find best-fit values <2.3, <3.0 and <3.5 keV for 68%, 95% and 99.7% probabilities respectively. We conclude that the spectrum of XRF 040916 is extremely soft compared to that of typical GRBs.

Redshift Estimation

This burst is extremely soft and this softness could be explained if XRF 040916 were a high-redshift GRB. To check this hypothesis, we first estimated the redshift from the Amati relation [6] using the 1st peak data. Assuming this relation, it is possible to estimate the redshift using only the flux and $E_{\rm peak}$ of a burst. We calculated $E^{\rm rest}_{\rm peak}$ and $E_{\rm iso}$ from the spectral parameters of the 1st peak data assuming various redshifts. As shown in Figure 2, the lower the redshift is, the more consistent are the computed values

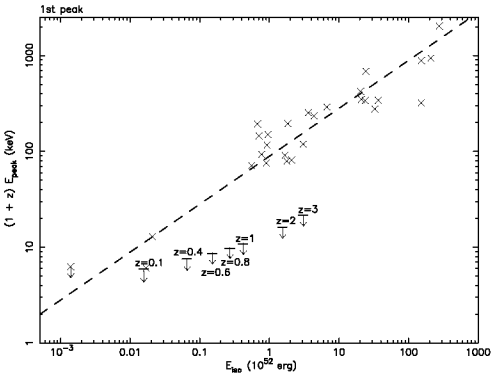

FIGURE 2. The ($E_{\rm iso}$-$E^{\rm rest}_{\rm peak}$) -plane for the 1st peak. The bars are for XRF 040916 at various distances. The crosses are the *BeppoSAX*-GRBs and *HETE-2* GRBs. The dashed line is the equation, $E^{\rm rest}_{\rm peak} = 89(E_{\rm iso}/10^{52}\ {\rm ergs})^{0.5}$ keV given by [6].

with the Amati relation. This result is also consistent with the Subaru redshift constraint of $z < 3$, imposed by its detection of the optical afterglow in the B-band [4].

We have also computed an upper limit to the pseudo-redshift (with the method described in [7]) using the WXM spectrum for the most intense 15 s long part of the 1st peak. To do this, we derived the upper limit to $E_{\rm peak}$ using the *constrained* Band model to fit the data. We find that $E_{\rm peak} < 6.2$ keV with 90% confidence, leading to a pseudo-redshift < 0.7, consistent with the preceding results. Thus we can reject a high redshift for this burst.

Origin of the 2nd peak

We can regard the 2nd peak as the rebrightning component. But its origin is not clear, and then the 2nd peak could be the following cadidates, (1) beginning of the afterglow (2) ambient density fluctuations of the X-ray afterglow, (3) patchy shell, (4) refreshed shock and (5) long-acting engine model.

First, we consider the possibility of (1) the beginning of the afterglow. This spectral and temporal evolution of the afterglow is caused by fireball evolution which takes place in the interstellar medium [8]. In this cases, the decay time of a late X-ray burst (i.e. afterglow) is supposed to be proportional to $\sim t^{-1}$ [9]. If we set the zero time (t_0) of the emission episode for the 1st peak, then the decay time of the 2nd peak is proportional to $t^{-12.7\pm0.3}$ in 2−25 keV energy band. Then this result is inconsistent with the above afterglow model.

For (2) the ambient density fluctuations of the X-ray afterglow model, this model explains afterglow variabilities by ambient density fluctuations caused by turbulence in the interstellar medium or variable winds from the progenitor star. If XRF 040916

was in the afterglow stage when the 2nd peak occurred, we can use a kinematical upper limit on the variability given by [10]. By the calculation using [10], we found that the observed variability exceeds the maximum allowed value, then ambient density fluctuations cannot explain the nature of the 2nd peak.

For (3) the patchy shell model, the variability timescale Δt of the afterglow at time t must be $\Delta t \geq t$ [11]. The patchy shell model cannot make a bump with variability timescale $\Delta t \sim 60$ s, which is shorter than the observed timescale $t \sim 370$ s. Furthermore, the flux of the 2nd peak is as bright as that of the 1st one. If this burst is explained by the patchy shell model, we must assume very large shell non-uniformity. Therefore we can marginally reject this model from the point of view of the variability timescale.

For (4) the refreshed shock model, multiple shells are ejected at various velocities, and the variability occurs when the slow inner shell catches up with the fast outer shell a long time later, since the velocity of the outer shell decreases through the ambient medium [12]. This model can not explain the flux variability of the 2nd peak because refreshed shocks cannot produce changes of more than 1 order of magnitude [13].

For (5) the long-acting engine model, at the observed time t, the central engine is still active and emitting shells. This can explain variability timescales down to a millisecond and there is no restriction on the flux variability. The most likely explanation of the 2nd peak is therefore the long-acting engine model. Furthermore, we considered curvature effect [14]. This effect occurs when the observer receives the progressively delayed emission from higher latitudes. The formula $F_\nu(t) = A[(t-t_0)/t_0]^{-(1+\beta)}$ represents the curvature effect, where β is the X-ray photon index during the decay, t_0 is the time zero point of the emission episode related to decay and A is a normalization parameter for the decay component. From fitting analysis, we found that the time zero point t_0 = -34.8 $\pm$ 34.9 s meaning that t_0 corresponded to the time zero point for the 2nd peak. This result implies that the zero time for the 1st peak doesn't coincide with the 2nd peak one; then the central engine was reactivated. Only this model can explain both the variability timescale and the flux variability for the 2nd peak. This event is similar to the Swift bursts XRF 050406 and GRB 050502B which are explained by the long-acting engine model [1].

REFERENCES

1. D. N. Burrows, et al., *Science* **309**, 1833–1835 (2005).
2. M. Arimoto, et al., *PASJ* **59**, 695–702 (2007).
3. Y. Yamamoto, et al., *GRB Coordinates Network* **2713**, 1 (2004).
4. G. Kosugi et al., *GRB Coordinates Network* **2730**, 1 (2004).
5. T. Sakamoto, et al., *ApJ* **602**, 875–885 (2004).
6. L. Amati, et al., *A&A* **390**, 81–89 (2002).
7. A. Pélangeon, et al., *AIP Conference Series* **836**, 149–152 (2006).
8. L. Piro, et al., *ApJ* **623**, 314–324 (2005).
9. R. Sari, T. Piran, and R. Narayan, *ApJL* **497**, L17 (1998).
10. K. Ioka, S. Kobayashi, and B. Zhang, *ApJ* **631**, 429–434 (2005).
11. E. Nakar, and Y. Oren, *ApJL* **602**, L97–L100 (2004).
12. M. J. Rees, and P. Meszaros, *ApJL* **496**, L1 (1998).
13. J. Granot, E. Nakar, and T. Piran, *Nature* **426**, 138–139 (2003).
14. E. W. Liang, et al., *ApJ* **646**, 351–357 (2006).